TEN YEARS
OF ATOMIC FORCE MICROSCOPY IN GLASS RESEARCH

HERVÉ ARRIBART, DANIEL ABRIOU

Laboratoire mixte CNRS/Saint-Gobain, Saint-Gobain Recherche, BP 135
39, quai Lucien Lefranc, 93303 Aubervilliers, France
E-mail: herve.arribart@sgr.saint-gobain.com

INTRODUCTION

The Atomic Force Microscope (AFM) was invented in 1986 by Binnig, Quate and Gerber [1], following on from the invention of the Scanning Tunneling Microscope (STM), which earned Binnig and Rohrer [2] the Nobel Prize in 1986. In some publications, the AFM is named SFM (Scanning Force Microscope) as well. In contrast with STM, AFM does not require the sample to be electrically conductive, an essential characteristic in the context of glass research. Principles of operation, experimental methodologies and description of possible artifacts can be found in many textbooks and review articles (see for example reference [3]).

The cardinal attribute of STM and AFM is that they allow for the observation and imaging of some solid surfaces at the atomic scale. "Seeing" individual atoms is more tractable with STM than with AFM (it was only in 1993 that "true atomic resolution" was attained with an AFM [4]), and it is not in any case an easy task. At first, this requires a sample with an extremely smooth surface, such as the atomically flat crystallographic faces found on single crystals. For this reason, AFM has seldom been used to study the atomic structure of glasses. But, the capability of imaging surfaces in the size range from <1 to 50 nm, which is much less demanding, and which was hardly achievable on insulating materials using other experimental techniques, was very attracting because this is the relevant scale for a number of scientific and technological glass problems. The first study on the utilization of the AFM in the context of glass research was presented by our laboratory in 1991. It shows images recorded at a resolution of 1 nm of the air and tin sides of float glass, of polishing grooves and defects, and of tin oxide coatings [5]. From that time, several hundred papers have reported research works on glass itself or on coatings deposited on glass.

The present paper reviews the first decade of use of Atomic Force Microscopy in glass research. During this period, the technique has been continuously upgraded. The basic principle of AFM is to measure the force experienced by a very sharp tip under the action of intermolecular interactions with atoms of the sample surface. In the original and most conventional operation mode, the tip stays in contact with the sample surface and is scanned over the area to analyze under the control of a computer. An image, where each pixel indicates the magnitude of the tip-surface interaction, is built by the computer, giving a topographic map of the sample surface. The AFM is rather easy to operate and very versatile. Generally, it does not require complicated sample preparation procedures. It can be operated with the sample placed in various environments, including under vacuum or immersed in a liquid. New modes of operation have progressively been introduced, such as the "intermittent-contact mode" (or "tapping mode") where a vibration of the tip perpendicular to the sample surface is superimposed to the scanning, so that at the bottom of its travel it just barely hits, or "taps" the sample. The "tapping mode" aims at getting a topographic image of the surface, too. Other affiliated methods have the purpose of mapping the distribution of a specific physical parameter of the surface:

- lateral force microscopy, or "friction force microscopy", which maps the lateral force experienced by the tip during scanning.
- force modulation microscopy and phase contrast microscopy, which measure the local elastic properties. They map the viscous or plastic dissipation of the sample due to the tip contact, and can therefore be interpreted in terms of hardness and softness.
- electrostatic force microscopy, which maps the surface charge distribution.
- magnetic force microscopy, which maps the magnetic susceptibility of the sample surface. The tip is then made of a ferromagnetic substance.

It is also possible with an AFM to perform local measurements of the surface acid-base character [6], of the tip-surface adhesion force [7], …

The two main drawbacks of AFM and affiliated techniques are the limited field of view and the possibility of artifacts coming from spurious interactions between the tip and the sample

Unless otherwise stated, examples discussed below deal with topographic images, that correspond to most of the research effort in glass research. Previous reviews of AFM imaging in glass research were published in 1996 [8] and 1997 [9].

GLASS

Glass structure

Atomic structure

As mentioned in the introduction, the hope to get atomically resolved AFM images is slighter with amorphous materials than with single crystals, due to the absence of crystallographic faces. It is only very recently that small humps that can be attributed to single atoms have been observed on amorphous materials. This was achieved, at first, on a metallic glass surface, using a STM [10], and secondly, on the fracture surface of a Ba-Si-O-C insulating amorphous compound, using an AFM [11]. The first atomically resolved AFM imaging of a silicate glass, a barium silicate in this case, was achieved last year [12]. Hexagonal rings visible on the images consist of six SiO_4 tetrahedra distant from each other by 0.26 nm, i.e. the length of a siloxane bridge. This result is very stimulating, because it opens the hope of a possible direct determination of the structure of glass.

Heterogeneity at the nanometer scale

There are more and more experimental indications that glasses are heterogeneous at the scale of a few nanometers [13, 14]. This heterogeneity can be seen as density fluctuations in pure silica, or as composition fluctuations in glasses of complex formulation. It is tempting to assume that the surface of easy cleavage in glass fracture reveals the structural heterogeneity. Careful AFM observations of the fracture surface of float glass at high resolution in the mirror zone, where the surface is very smooth, have therefore been carried on. They show a surface made of small hillocks, a few tens nanometers wide and about one nanometer high [15,16]. Similar features were observed on the fractured surfaces of E glass fibers [17], of pure silica [15] and of a fluoride glass [15], and it seems that they also exist in non devitrified $Li_2O.2SiO_2$ glasses [18]. Furthermore, a fractal analysis of the topography of the fracture surface of float glass, to be described below, shows the existence of a characteristic length of a few nanometers, that varies only slightly with the crack velocity [19, 20], and w hich could be interpreted as the characteristic dimension of the heterogeneity. The reason for the discrepancy by almost one order of magnitude between the heterogeneity scale inferred from spectroscopic and diffraction techniques [13, 14] and that inferred from AFM studies would remain to understand.

Recrystallization and phase separation

The AFM observation of fracture surface also provides a mean to study the heterogeneity due to recrystallization or phase separation in glasses. Precursor signs of crystallization were thus detected in a metallic glass [21]. Nucleation and crystallization in glasses of various compositions (lithium silicate [18], borosilicate [20], fluoride glass [22]), precipitation of metallic nanocrystals in a bismuth doped silicate glasses reduced in hydrogen atmosphere [23], and organic-inorganic phase separation in a polymer-silica hybrid material [24] have been studied in the same manner. The observation of the external surface also provided a way to follow the microstructural evolution of glass-ceramics at different stages of the crystallization [25]. It has also served to detect the formation of iron nanoparticules in ion-implanted silica [26].

Roughness and surface defects

AFM is a peerless way of performing surface height measurements with a precision better than 0.1 nm and over lateral scales from a few tenths nanometers to 100 mm. It has therefore become common to use AFM as a tool of evaluation of the quality of a glass surface. Detection of surface defects and measurements of surface roughness are amongst the most frequent AFM utilizations in research on glass and coatings.

Roughness measurements

Surface roughness is not an easy parameter to measure, because its value depends on the lateral scale of the height measurement. It is therefore a spectral parameter, that must be defined by its spectral density as a function of the lateral wavenumber (for a simple introduction to this problem, see reference [27]). Consequently, a roughness value is meaningful only if the lateral scale and the lateral resolution of the instrument are given, because these two parameters define the bandwidth of the measurement. The figure that is generally reported in the literature is the roughness root-mean-square (rms) value. Details of correct measurement methods of the roughness spectral density can be found in references [28-30]. Reference [31] explains in a very detailed manner how to use an AFM for rigorous height profile measurements and what are the (manifold) possible artifacts. Several comparisons of roughness measurements by AFM and by other methods (mechanical profiler [27-29, 32], optical profiler [28, 29, 32, 33], total integrated light scattering[33], X-ray scattering [30]) have been published. Among all these methods, AFM, by far, gives access to the largest wavenumbers (i.e. the smallest lateral dimension), and the quantitative comparison with other techniques is possible only at scales where bandwidths overlap. In all reports mentioned above, the agreements are good, if not excellent.

Surfaces of industrial glasses

As-produced industrial glasses have remarkably smooth surfaces, probably because they result from the cooling of a liquid surface, without contact with any tool. Small defects are sometimes observed on the surface of float glass [5] and fiberglass [15, 34], but AFM is not a reliable method for systematic detection because of its small field of view. At the scale of one micrometer, the typical rms roughness of the air and tin sides of a clean and fresh sample of float glass is 0.2 nm [5]. The roughness of glass fibers is difficult to define in a rigorous manner, because of the existence of waviness along the length of the fiber [35, 36]. It is proposed that this waves have origin in the fiberizing process [35]. If their profile is substracted by the computer, the residual rms roughness is found as low as 0.1 nm for a 1 mm lateral scale [5]. The roughness spectral density of a float glass surface was measured on a very wide bandwidth, from 1 nm to 3 mm (AFM was used in the 1 nm – 100 μm range, and a mechanical profiler in the 1 μm – 3 mm range). Remarkably, it is found that over this 6.5 decades range the dependence follows a power law [27], which means that the surface is self-affine : it is kept invariant by the transformation $(x, y, z) \rightarrow (\lambda.x, \lambda.y, \lambda^{\zeta}.z)$, where ζ is a scaling factor, measured to be 0.36, and z is the direction normal to the surface. The explanation of this behavior remains to find.

Polishing

Because new optical applications require a rms roughness in the sub-tenth of nanometer range, and because the size of polishing grains is sub-micronic, AFM has become a familiar method of evaluation of the quality of polished glass surfaces [31]. Glass surfaces polished in a conventional manner are characterized by scratches and grooves in which abrasive particles sometimes remain imbedded [5, 31, 37-39]. Both defects significantly contribute to the measured roughness. This is not the case with superpolishing which leads to rms roughness values as small as 0.06-0.09 nm, measured at a lateral scale of a few tens micrometers [28, 31, 33]. Clearly, mechanical abrasion is not alone at work in superpolishing. Various other surface treatments have been tested to smoothen glass substrates. With AFM, it has been shown that a silica glass surface exposed to ion-irradiation is roughened for low doses and smoothened for high doses [40], and that a glass substrate exposed to a N_2-H_2 plasma can be significantly smoothened [41].

Corrosion and aging

It is well known that glass surfaces are generally not stable against water and humidity. The results of the evolution depend on the glass composition [42]. Cleaning a glass substrate is not without consequence on the surface chemical composition, even if the topography is not altered [43]. The first step of the corrosion process is the formation of an adsorbed water layer, as confirmed by Rudd et al. in an experiment where adhesion between the AFM tip and the glass surface is measured [44]. AFM is an appropriate tool for imaging the topographic changes of glass surfaces undergoing corrosion by the attack of ambient air and aqueous solutions as well. Furthermore, the observation can be performed *in situ*. However, the method has also some inherent drawbacks. Firstly, the field of view is small, posing the problem of the statistical significance of the observed details. Secondly, in the usual "contact" and "tapping" modes of imaging, the tip of the instrument is in permanent or intermittent contact with the sample surface, possibly causing imaging artifacts or damages to the fragile altered surface layer. Schmitz et al. have shown that images recorded in the "contact mode", the "tapping mode" and by "phase imaging" (a kind of force modulation microscopy) do not stress the same surface features [45-47]. With the latter, it is possible to distinguish between soft regions, e.g. where a gel layers is present, and hard regions [47].

In spite of the difficulties mentioned above, many studies on corrosion and aging of glasses of various compositions in various environments have been reported [15, 34, 45-53]. In some of them, observations are performed starting from fresh fractured surfaces in order to guarantee the significance and reproducibility of the experiment [45-47, 52, 53]. These studies confirm known peculiarities of glass corrosion and bring new insights. As expected, glass surfaces are found stable in the absence of water [45,46], and the degradation of pure silica is much slower than that of alkali or alkaline-earth silicates [48, 52]. The effects of water in humid air or as a liquid phase are found different : characteristic pits develop in humid air, while the roughness increases in a more uniform way under water [46]. The corrosion process is non homogeneous at the sub-micron scale, and it is accentuated when corrosive gases, such as SO_2 and NO_2, are present [47]. In humid air, swelling and formation of a gel layer are the first observed effects with alkali silicates [45, 46, 48]. With alkaline-earth silicates, the formation of microcrystals characterizes the early stages of weathering [48,52]. As discussed in reference [48], this difference can be explained by the difference in ionic mobilities, which would cause the adsorbed water layers to be of different thicknesses. This set of works attests that AFM has an indisputable potential in glass corrosion studies. To push the technique at its best level, it is necessary that various mode of imaging are simultaneously used, that chemical analytical techniques are used in parallel in a more systematic way, and, above all, that different research groups working on samples of the same composition collaborate.

Fracture

It has early been realized that AFM and other scanning probe microscopies have a strong potential in research on glass fracture [34, 54, 55]. AFM has renewed the activity in fractography, and it has allowed

to improve significantly our understanding of fracture initiation and crack propagation in glass.

Fractography

AFM fractography has been discussed above in relation with glass structure and corrosion. But, it is well known that the analysis of the fracture surface can provide fruitful information on the fracture dynamics [56]. Fractography was traditionally based on the optical observation of three successive zones (namely mirror, mist and hackle), starting from the surface defect responsible from the fracture. It was therefore attracting to investigate the topography of these zones at a much shorter scale with AFM [15, 16, 57] or STM [54]. Although these works were not all conducted with samples of the same compositions nor broken in the same way, some common conclusions can be drawn. Firstly, passing from mirror to mist or from mist to hackle is not as discontinuous as it looks in optical fractography, and each zone presents a variation of topography in the radial direction (defined starting from the fracture initiation defect). In particular, the roughness increases continuously from the start to the end of the mirror zone [15, 16, 57, 58]. Secondly, images recorded in the hackle zone show some self-similarity [15, 16, 54], which is interpreted in terms of micro-branching of the fracture front. At each micro-branching, a micro-mirror zone is observed, which suggests that the crack velocity is not uniform in this zone. This self-similarity has been analyzed using fractal geometry [54, 57]. The different studies, which have been reported, also present some discrepancies. In particular, the mirror zone is found perfectly isotropic in some of them [15, 16, 59], while it shows a pattern related with the direction of crack propagation in others [54]. This can be due to non- equivalent modes of fracture.

AFM experiments have been performed on fractured surfaces of soda-lime glass resulting from crack propagation at a controlled velocity with a four points bending system [17, 19]. A fractal analysis of the roughness was performed (see chapter Rougheness and suface defects). It leads to the finding that the fractured surface is not self-affine but is characterized by two regimes. At large lateral length (small wavenumber), the roughness exponent is 0.78, and it is 0.50 at small length (large wavenumber). Both values are inde-pendent on the crack velocity. A crossover length, which slightly depends on the velocity, separates the two regimes. The experiment was also performed with an intermetallic alloy, providing the same result and the same numerical values of the roughness exponents. Although this result is not satisfactory interpreted, it has a major importance, because the universality of the roughness exponent of fractured surface is the subject of an active discussion [60-62].

Crack initiation

In order to explain the experimental values of the mechanical strength of glass, it is generally assumed that localized microscopic surface flaws should exist at the surface, which would act as stress concentrators. The hypothesis sounds reasonable, not only because it comes as an extrapolation of macroscopic data [63], but also because the random distribution of the size of these defects could explain the Weibull statistics which prevails to interpret the fracture of glass fibers. However, many attempts to visualize these defects with AFM have failed [15, 17, 55]. An alternative explanation can be found in the surface topography of virgin fibers. As in the case of float glass [27], the roughness is found to be self-affine (see chapter Surfaces of industrial glasses) [17]. As suggested in reference [64], roughness fluctuations could act as the stress concentrators. From a theoretical point of view, the fractal approach has been used to derive the Weibull distribution of fracture stress [17, 65].

Observation of static and propagating cracks

It has turned to be possible to observe with AFM the far end of a crack tip during propagation [15, 17, 66-68]. From a quantitative analysis of the surface topography during propagation and after it came to stop, it was concluded that a non-(linear elastic) deformation, probably a plastic deformation, occurs in soda-lime glass in the close vicinity of the crack tip [66, 68]. On the contrary, pure silica does not depart from its purely elastic behavior. The difference could be explained by sodium ions migration, driven by the mechanical stress, in the core region of the crack [17]. Kinetic fracture of glass in the sub-critical regime has also been studied at the nanometer scale [67], in humid and wet air, and under pure water. The role of humidity on crack propagation was confirmed [67]. The crack velocity was measured as a function of the mechanical-energy-release rate G. Experiments conducted at extremely low velocities, below 10^{-13} m s^{-1}, provided evidence for the existence of a threshold load for crack propagation [67]. As expected, the threshold value of G is found to be smaller in ambient atmosphere (1.5 J m^{-2}) than in water (< 0.8 J m^{-2}). The question of the existence or not of a threshold has remained controversial for a long time, because the very low velocity regime was hardly possible to investigate before the advent of AFM.

Adhesion of polymers and other materials to glass

When an interface fails, the failure can be either interfacial or cohesive. The failure front propagates strictly between the two materials in the former case, while one of them yields in the vicinity of the interface in the latter. Identifying the locus of failure is very instructive, because it tells if the adhesion weakness lies in the interfacial bonds or in the cohesive strength of the materials. This is a problem of both practical and fundamental interests, that AFM can readily solve. With glass/polymer systems, it is easy to determine if some polymer residues are present on the surface of the

debonded glass surface [69]. It is even possible to resolve intricate situations when a cohesive failure occurs at a molecular distance from the interface, a failure mode called "quasi-interfacial". The adhesion failure between glass (soda-lime silicate or pure silica) and a polyurethane elastomer revealed that the different modes of failure can occur, depending on the composition of glass and on the conditions of aging of the interface [69]. Here again, the role of sodium ions in glass is crucial. In a PVC/glass joint made with a thin adhesive layer, the same approach lead to the conclusion that the locus of failure is primary at the glass/adhesive interface [70]. On the glass/polyurethane system, optical and AFM observations of the pattern formed by polymer remaining on glass lead to a description of the mechanical response of the elastomer at the failure front [71, 72]. In particular, the formation of voids in the polymer just in front of the failure line was evidenced. The same approach was used to study glass/PDMS (polydimethylsiloxane) adhesion [73]. In other studies, it is the surface of the polymer that was debonded from the glass substrate, which is examined [74]. The same method has been applied to a metal/glass interface, leading again to the conclusion that voids are formed, by plastic deformation of the metal [75].

In a completely different approach, promising attempts to image with an AFM working in AC mode the mechanical response of the interphase between a reinforcement glass fiber and the surrounding polymeric matrix have been published [76]. The sample used in that study was a cross section of a model composite sample.

COATINGS ON GLASS

AFM instruments are now commonly found in laboratories working on thin films. They are generally used in association with analytical surface spectroscopies, such as XPS (X-ray Photo-emission Spectroscopy) and SIMS (Secondary Ion Mass Spectroscopy). Field-Emission Scanning Electron Microscopy (FE-SEM) begins to compete with AFM, since it has high resolution capabilities without the mandatory necessity of sample metallization, which is necessary with a traditional SEM. Nevertheless, the role of AFM is still increasing, as figure 1 shows: it gives the evolution since 1992 of the proportion of articles published in the journal "Thin Solid Films" in which at least one AFM image is displayed. We have not held the same statistics with the journal "Langmuir", which is devoted to the surface and the deposition of organic materials, but the general trend clearly is the same. We estimate that the total number of papers dealing with organic or inorganic coatings on glass, in which use of AFM is reported is about two hundred. We discuss below research works that seem to us representative of AFM capabilities.
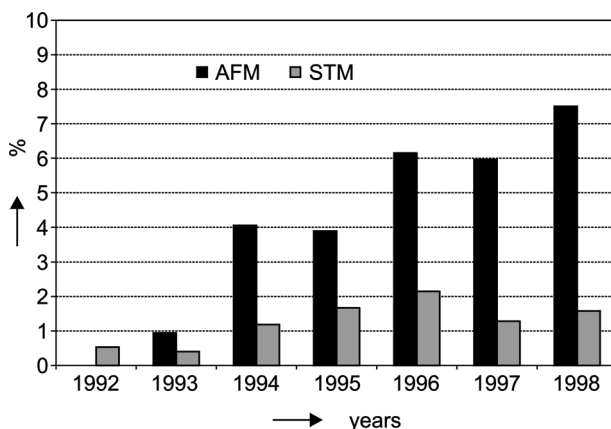

Figure 1. Proportion of research articles published in the journal "Thin Solid Films" in which at least one AFM image is displayed. The same statistics for STM is given for comparison.

Inorganic coatings

Microstructural characterization

AFM topographic images characterize the morphology of coatings. Combined with X-ray diffraction results, they give relevant information about the amorphous or crystalline form of the coating. This information helps to understand the growth mechanism and to determine the best parameters of deposition or post-treatment. Interesting recent examples are reported in relation with the deposition of doped zinc oxide films by reactive sputtering [77], vacuum-evaporated tin oxide thin films [78], zinc sulfide thin films grown by atomic layer epitaxy [79], indium-tin oxide deposited by sputtering from a metallic or an oxide target [80], crystallization of titanium oxide thin films during annealing treatment [81], damages produced by tungsten doping of vanadium oxide by ion implantation and subsequent recrystallization [82], and lead sulphide thin films grown by deposition from liquid solutions [83]. The latter paper shows that instructive information on the surface coverage and the presence of contaminants are gained from lateral force microscopy and force modulation spectroscopy, besides usual AFM. It has also been proposed to use AFM on cross-sections of the coating [84]. The technique was recently used with a silica-coated glass substrate [85].

Coating roughness

The optical response of a coated glass can be significantly affected by the roughness of the coating. The understanding of the parameters that control the roughness is therefore a subject of research works. Height measurement and roughness analysis techniques are the same as described in chapter Roughness and surface defects. Typical examples can be found in the context of CVD deposition of fluoride doped tin oxide on float glass [86], deposition of chromium films by oblique sputtering [87], thermally evaporated manga-

nese fluoride films [88], reflecting copper films deposited by partially ionized beam deposition[89]. It was also shown that an argon ion irradiation post-treatment used to improve the adhesion between gold films and glass has the undesired consequence to significantly increase the roughness [90]. Roughness measurements on coatings made by sol-gel give information on the densification of the material during the thermal treatment or other post-treatment [39, 91]. Interestingly, it was found that sol-gel coating a rough glass substrate can have a smoothening effect [92].

Corrosion of coatings

A few papers report the use of AFM to follow the evolution of some inorganic coatings in corrosive environments, for example titanium oxide film, crystallized or amorphous, in a NaOH solution [93], or chromium doped zinc oxide in various acid solutions [94]. It seems to us that the potential of AFM in this matter is not sufficiently exploited.

Organic coatings

Langmuir-Blodgett and self-assembled layers

The deposition of a monomolecular layer of organic molecules is an elegant way to functionalize glass surfaces. Historically, Langmuir-Blodgett films have been developed at first. With this technique, the layer is very well organized. The molecules form a two-dimensional crystal at the substrate surface. In some cases, it is possible to image this molecular structure by AFM, even when it is deposited on a non atomically flat substrate like amorphous silica [95]. A serious drawback of Langmuir-Blodgett films is their lack of durability, due to the absence of chemical bonding with the substrate. This was improved with the advent of self-assembled layers [96]. With this technique, each molecule can be attached with covalent bond to the silica substrate. Many research groups study how to functionalize glass surfaces in this way, mainly with the purpose to get hydrophobic or hydrophilic surfaces. An unique attribute of AFM in that matter is that it can follow *in situ* the growth of the layer [97, 98]. These experiments, performed with a silica-coated silicon wafer, lead to a clear understanding of the organization of the layer at the different stages of the process. They also gave a confirmation and an explanation for the determinant role of the solution temperature on the quality of the layer. Ex situ experiments performed with borosilicate glass [99] or float glass [100] substrates lead to conclusions about the layer formation mechanisms, which are compatible with the *in situ* experiments.

Fibers coatings and sizings

AFM observations of coated optical fibers can help to the understanding of the aging process and to the formulation of the coating in relation with mechanical strength [101,102]. The addition of nanosized particles of silica to the polymer coating has been shown to improve long-term mechanical properties, a fact that the AFM analysis has shown to be due to the suppression of surface dissolution [101]. AFM observations of E glass reinforcement fibers coated with various coupling agents or sizings of various formulations have also been made [103, 104].

Functional polymer coatings

AFM is an appropriate tool to investigate the so-called superhydrophobic coatings that can be obtained by combining polymer chemistry and surface morphology tailoring. Two different strategies are adopted: deposition of the hydrophobic layer on a textured sol-gel coating [105], or one-step deposition of a textured polymer layer, for example by ion-plating [106], or by plasma-enhanced CVD [107]. Many examples of utilization of AFM for the characterization of polymer layers with optical functionality, such as electroluminescence[108,109], can be found.

The problem of self-dewetting

Polymer layers, especially those deposited from a liquid phase (as in spin casting or dip coating), often have low viscosity. Under the action of surface and interfacial tension, self-dewetting is then possible. It leads to the formation of droplets or other patterns that AFM can image, thanks to the daintiness of its interaction with soft matter. Such behavior has been detected in the following cases: polyethyleneglycol monolayer on silica[110], perfluoroalkyl methacrylate films on glass [111], polymethylmetacrylate on soda-lime glass and pure silica [112]. Interestingly, in the latter case, dewetting arose on soda-lime glass but not on silica. Dewetting of sizing layers at the surface of E-glass fibers has also been evidenced [104], posing a problem of practical interest.

CONCLUSION

This review shows that AFM, together with affiliated scanning microscopies, can address many different problems of glass science and technology. It has to be considered both as an analytical tool and as a research instrument.

Because it is versatile and relatively easy to operate, AFM is appropriate for the observation of the morphology of surfaces of glass and coatings and for the evaluation of their quality in terms of defects and roughness. But, for glass surfaces and inorganic coatings, the recently introduced Field-Emission Scanning Electron Microscope may be preferred because of the absence of almost any artifact and because the field of view is wider. The interaction of the AFM tip with the sample, that is an inherent factor of the technique, is a source of artifacts that need experience to be avoided. In the case of soft matter, such as liquids or low viscosity organic layers, the AFM has no competitor. AFM is also the only instrument advisable for rigorous roughness measurements at lateral scales below 100 nanometers.

The capacity for in situ observations in a wide diversity of environments, from ultra-high vacuum to liquid medium, places AFM on the first rank among experimental techniques for the study of corrosion and aging. We expect the activity in that field to grow.

AFM still has a strong potential in basic research on glass. We can expect that it will play a major role in the determination of the structure of glass at the atomic and mean-range scales, and in the understanding of atomistic and dissipation mechanisms involved in glass fracture and in glass-polymer adhesion as well.

References

1. Binnig G., Quate C.F., Gerber C.: Physical Review Letters *56*, 930 (1986).
2. Binnig G., Rohrer H.: Helvetica Physica Acta *55*, 726 (1982).
3. http://www.park.com/spmguide/contents.htm.
4. Ohnesorge F., Binnig G.: Science *260*, 1451 (1993).
5. Creuzet F., Abriou D., Arribart H.: Proceedings of the first conference of the European Society of Glass Science and Technology, p.111, Sheffield 1991.
6. Lin X.Y., Creuzet F., Arribart H.: Journal of Physical Chemistry *97*, 7272 (1993).
7. Hoh J.H., Cleveland J.P., Prater C.B., Revel J.P., Hansma P.K.: Journal of the American Chemical Society. 4917 (1992).
8. Zarzycki J.: Journal of Non-Crystalline Solids *196*, 7 (1996).
9. Rädlein E, Frischat G.H.: Journal of Non-Crystalline Solids *222*, 69 (1997).
10. Schaub T.M., Bürgler D.E., Schmidt C.M., Güntherodt H.J.: Journal of Non-crystalline Solids *205-207*, 748 (1996).
11. Raberg W., Lansmann V., Jansen M., Wandelt K.: Angew. Chem. Int. Ed. Engl. *36*, 2646 (1997).
12. Raberg W., Wandelt K. : Applied Physics *A 66*, S1143 (1998).
13. Gaskell P.H.: Journal of Non-Crystalline Solids *222*, 1 (1997).
14. Greaves G.N., Smith W., Giulotto E., Pantos E.: Journal of Non-Crystalline Solids *222*, 13 (1997).
15. Guilloteau E.: *La fracture du verre: phenoménes-clés á l'échelle nanométrique*, Thése, Université d'Orsay, 1995.
16. Guilloteau E., Arribart H., Creuzet F.: Mat. Res. Soc. Symp. Proc. *409*, 365 (1996) .
17. Nghięm B.: *Fracture du verre et hétérogénéités á l'échelle submicronique*, Thése, Université Paris VI, 1998.
18. Schmidt A., Frischat G.H.: Physics and Chemistry of Glasses *38*, 161 (1997).
19. Daguier P., Nghięm B., Bouchaud E., Creuzet F.: Physical Review Letters *78*, 1062 (1997) .
20. Nghięm B., Arribart H., Creuzet F.: Fundamental of Glass Science and Technology – proceedings of the 4th ESG Conference, p.33 Vaxjö 1997.
21. Watanabe Y., Nakamura Y.: Journal of Materials Science Letters *11*, 1534 (1992).
22. Anselm L., Frischat G.H.: Journal of Non-Crystalline Solids 217, 115 (1997) .
23. Czajka R., Trzebiatowski K., Polewska W., Koscielska B., Kaszczyszyn S., Susla B.: Vacuum *48*, 213 (1997).
24. Wei Y., Jin D., Brennan D.J., Rivera D.N., Zhuang Q., DiNardo N.J., Qiu K.: Chem. Mater *10*, 769 (1998).
25. Diaz C., Vazquez M., Marco J., Caballer V., Rincon J.M., Romero M.: Proceedings of the 17th International congress on Glass, p.160, Beijing 1995.
26. Bukharaev A.A., Janduganov V.M., Samarsky E.A., Berdunov N.V.: Applied Surface Science *103*, 49 (1996).
27. Abriou D., Levillain Y., Arribart H., Creuzet F. : Proceedings of the International Symposium on Glass Problems, p.427, Istanbul 1996.
28. Ringel G., Kratz F., Schmitt D-R., Mangelsdord J., Creuzet F., Garratt J.: SPIE *2536*, 317 (1995) .
29. Poon C.Y., Bhushan B.: Wear *190*, 89 (1995).
30. Asadchikov V.E., Duparré A., Jakobs S., Karabekov A.Y., Kozhevnikov I.V., Krivonosov Y.S.: Applied Optics *38*, 684 (1999).
31. Bennett J.M., Jahanmir J. Podlesny J.C., Balter T.L., Hobbs D.T.: Applied Optics *34*, 213 (1995).
32. Poon C.Y., Bhushan B.: Wear *190*, 76 (1995).
33. Duparré A., Jakobs S.: Applied Optics *35*, 5052 (1996).
34. Creuzet F., Guilloteau E., Arribart H.: Second ESG Conference, p.163 Venice 1993.
35. Curtin Carter M.M., McIntyre N.S., Davidson R., King H.W.: J. Vac. Sci. Technol. *B 14*, 1867 (1996).
36. Abriou D., Arribart H., unpublished results.
37. Meyer E., Haefke H., Güntherod H-J., Anderson O., Bange K.: Glastech. Ber. *66*, 30 (1993).
38. Hu Y.Z., Gutmann R.J., Chow T.P., Witcraft B.: Thin Solid Films *332*, 391 (1998).
39. Rädlein E., Ambos R., Frischat G.H.: Fresenius J. Anal. Chem. *353*, 413 (1995).
40. Oyoshi K., Hishita S., Wada K., Suehara S., Aizawa T.: Applied Surface Science *100/101*, 374 (1996).
41. Moniruzzaman S., Inokuma T., Kurata Y., Takenaka S., Hasegawa S.: Thin Solid Films *337*, 27 (1999).
42. Hench L.L., Clark D.E.: Journal of Non-Crystalline Solids *28*, 83 (1978).
43. Couillard J.G., Ast D.G., Umbach C., Blakely J.M., Moore C.B., Fehlner F.P.: Journal of Non-Crystalline Solids *222*, 429 (1997).
44. Rudd G.I., Garofalini S.H., Hensley D.A.: J. Am. Ceram. Soc. *76*, 2555 (1993).
45. Schmitz I., Schreiner M., Friedbacher G., Grasserbauer M.: Anal. Chem. *69*, 1012 (1997).
46. Schmitz I., Prohaska T., Friedbacher G., Schreiner M., Grasserbauer M.: Fresenius J. Anal. Chem. *353*, 666 (1995).
47. Schmitz I., Schreiner M., Friedbacher G., Grasserbauer M.: Applied Surface Science *115*, 190 (1997).
48. Watanabe Y., Nakamura Y., Dickinson J.T., Langford S.C.: Journal of Non-Crystalline Solids *177*, 9 (1994).
49. Trens P., Denoyel R., Guilloteau E.: Langmuir *12*, 1245 (1996).
50. Marshall J.D., Josefowicz J.Y., Ducheyne P.: Bioceramics *6*, 390 (1993).
51. Sato A., Tsukamoto Y.: Journal of the Ceramic Society of Japan *101*, 400 (1993).
52. Curtin Carter M.M., McIntyre N.S., King H.W., Pratt A.R.: Journal of Non-Crystalline Solids *220*, 127 (1997).
53. Larson E.D., Pye L.D., Rädlein E., Frischat G.H., Weeks R.A.: Chem. Erde *56*, 423 (1996).

54. Kulawansa D.M., Jensen L.C., Langford S.C., Dickinson J.T.: J. Mater. Res. *9*, 476 (1994).
55. Guilloteau E., Hénaux S., Arribart H., Creuzet F.: Glastech. Ber. Glass Sci. Technol. *68 C1*, 271 (1995).
56. Varner J.R., Frechette V.D. edts.: *Fractography of glasses and ceramics, Advances in Ceramics 22*, The American Ceramic Society, 1986.
57. Wünsche C., Rädlein E., Frischat G.H.: Glastech. Ber. Glass Sci. Technol. *68 C1*, 275 (1995).
58. Wünsche C., Rädlein E., Frischat G.H. : Fresenius J. Anal. Chem. *358*, 349 (1997).
59. Moody N.R., Robinson S.L., Lucas J.P., Handrock J., Hwang R.Q.: J. Am. Ceram. Soc. *78*, 114 (1995).
60. Mandelbrot B., Passoja D.E., Paullay A.J.: Nature *308*, 721 (1984).
61. Bouchaud E., Lapasset G, Planés J.: Europhysics Letters *13*, 73 (1990).
62. Maloy K.J., Hansen A., Hinrichsen E.L., Roux S.: Physical Review Letters *68*, 213 (1992).
63. Griffith A.A.: Philos. Trans. R. Soc. London A *221*, 163 (1921).
64. Bouten P.C.P., de With G., J. Appl. Phys. *64*, 3890 (1988).
65. Anderson T.L.: Scripta Metallurgica *23*, 97 (1989).
66. Guilloteau E., Charrue H., Creuzet F.: Europhysics Letters *34*, 549 (1996).
67. Hénaux S., Creuzet F.: Journal of Materials Science Letters *16*, 1008 (1997).
68. Hénaux S., Creuzet F.: J. Am. Ceram. Soc., accepted for publication.
69. Creuzet F., Ryschenkow G., Arribart H.: Journal of Adhesion *40*, 15 (1992).
70. Vabrik R., Bertoti I., Czajlik I., Tury G., Keresztes Z., Ille A., Rusznak I., Vig A., Kalman E.: J. Adhesion Sci. Technol. *13*, 97 (1999) .
71. Ryschenkow G., Arribart H.: Journal of Adhesion *58*, 143 (1996).
72. Rémy P.: *Rupture d'adhésion sur le verre d'un polyuréthane de propriétés viscoélastiques déterminées*, Thése, Université Paris XI-Orsay, 1997.
73. Ryschenkow G., Remy P., Touraine S.: Le Vide, Les Couches Minces *272 suppl*, 90 (1994) .
74. Swadener J.G., Liechti K.M., de Lozanne A.L.: Journal of the Mechanics and Physics of Solids *47*, 223 (1999).
75. Nakahara S., Langford S.C., Dickinson J.T.: J. Mater. Res. *10*, 2033 (1995).
76. Munz M. Sturm H., Schulz E., Hinrichsen G.: Composites Part A *29A*, 1251 (1998).
77. Szyszka B., Jäger S.: Journal of Non-Crystalline Solids *218*, 74 (1997).
78. Man W.K., Yan H., Wong S.P., Wilson I.H., Wong T.K.S.: J. Vac. Sci. Technol. *3*, 1593 (1996).
79. Ihanus J., Ritala M., Leskelä M., Prohaska T., Resch R., Friedbacher G., Grasserbauer M.: Applied Surface Science *120*, 43 (1997).
80. Vollmers R., Rädlein E., Frischat GH.: Fundamental of Glass Science and Technology – 4ᵗʰ ESG Conference, p.23, Vaxjö 1997.
81. Martin N., Rousselot Ch., Rondot D., Palmino F., Mercier R.: Thin Solid Films *300*, 113 (1997).
82. Jin P., Nakao S., Tanemura S.: Thin Solid Films *324*, 151 (1998) .
83. Resch R., Friedbacher G., Grasserbauer M., Kanniainen T., Lindroos S., Leskelä M., Niinistö L.: Applied Surface Science *120*, 51 (1997).
84. Duparré A., Ruppe C., Pischow K.A., Adamik M., Barna P.B.: Thin Solid Films *261*, 70 (1995).
85. Rädlein E., Liu J. Hauk R., Frischat G.H.: Proceedings of the 18ᵗʰ International Congress on Glass, San Francisco 1998.
86. Urban III F.K., Ruzakowsky Athey P., Islam Md.S.: Thin Solid Films *253*, 326 (1994).
87. Le Bellac D., Niklasson G.A., Granqvist C.G.: Europhysics Letters *32*, 155 (1995) .
88. Ruppe C., Duparré A.: Thin Solid Films *288*, 8 (1996) .
89. Yoon Y.S., Kim K.H., Jang H.G., Jung H.J., Koh S.K.: J. Vac. Sci. Technol. A *14*, 2517 (1996).
90. Jang H.G., Kim K.H., Han S., Choi W.K., Jung H-j., Koh S.K., Kim H.B.: J. Vac. Sci. Technol. A *15*, 2234 (1997).
91. Ambos R., Rädlein E., Frischat G.H.: Glastech. Ber. Glass Sci. Technol. *68 C*, 351 (1995) .
92. Affatigato M., Osborne D., Haglund Jr. R.F.: Journal of Non-Crystalline Solids *181*, 27 (1995).
93. Yongjuan D., Rädlein E., Frischat G.H.: Proceedings of the International Symposium on Glass Problems, p.462, Istanbul 1996.
94. Shinoda M., Nishide T., Sawada Y., Hosaka M., Matsumoto T.: Jpn. J. Appl. Phys. *32*, L 1565 (1993).
95. Zhai X., Kleijn J.M.: Thin Solid Films *304*, 327 (1997) .
96. Maoz R., Sagiv J.: J. Coll. Interface Sci. *100*, 2 (1984).
97. Davidovits J.V., Pho V., Silberzan P., Goldmann M.: Surface Science *352-354*, 369 (1996).
98. Goldmann M., Davidovits J.V., Silberzan P.: Thin Solid Films *327-329*, 166 (1998).
99. Winger T.M., Chaikof E.L.: Langmuir *14*, 4148 (1998).
100. Banga R., Yarwood J., Morgan A.M., Evans B., Kells J.: Langmuir *11*, 4393 (1995).
101. Rondinella V.V., Matthewson M.J., Kurkjian C.R.: J. Am. Ceram. Soc. *77*, 73 (1994) .
102. Volotinen T.T., Yuce H.H., Frantz R.A.: SPIE *1973*, 161 (1993).
103. El Achari A., Ghenaim A., Wolff V., Caze C., Carlier E.: Textile Res. J. *66*, 483 (1996).
104. Ryschenkow G., unpublished results.
105. Akamatsu Y., Yamazaki S., Makita K., Inaba H., Kai Y.: Proceedings of the 18ᵗʰ International Congress on Glass, San Francisco 1998.
106. Veeramasuneni S., Drelich J., Miller J.D., Yamauchi G.: Progress in Organic Coatings *31*, 265 (1997).
107. Hozumi A., Takai O.: Thin Solid Films 303, 222 (1997).
108. Hanai N., Sumitomo M., Yanagi H.: Thin Solid Films *331*, 106 (1998).
109. Granström M., Inganäs O.: Advanced Materials *7*, 1012 (1995).
110. Nettesheim S., Zeisel D., Handschuh M., Zenobi R.: Langmuir *14*, 3101 (1998).
111. Sheiko S., Lermann E., Möller M.: Self-dewetting of perfluoroalkyl methacrylate films on glass, Langmuir *12*, 4015 (1996).
112. Berquier J.M., Creuzet F., Grimal J.F.: Langmuir *12*, 597 (1996).

Submitted in English by the authors.